ResearchGate

See discussions, stats, and author profiles for this publication at: https://www.researchgate.net/publication/224839046

Multiplex spectroscopy of stable and transient species in a molecular beam

ARTICLE *in* JOURNAL OF RAMAN SPECTROSCOPY · AUGUST 2007

Impact Factor: 2.67 · DOI: 10.1002/jrs.1735

CITATIONS
11

READS
32

6 AUTHORS, INCLUDING:

Marek Tulej
Universität Bern
99 PUBLICATIONS **726** CITATIONS
SEE PROFILE

Gregor Knopp
Paul Scherrer Institut
80 PUBLICATIONS **746** CITATIONS
SEE PROFILE

Peter Radi
Paul Scherrer Institut
127 PUBLICATIONS **1,442** CITATIONS
SEE PROFILE

Available from: Marek Tulej
Retrieved on: 25 January 2016

JOURNAL OF RAMAN SPECTROSCOPY
J. Raman Spectrosc. 2007; **38**: 1022–1031
Published online 12 June 2007 in Wiley InterScience
(www.interscience.wiley.com) DOI: 10.1002/jrs.1735

JRS

Multiplex spectroscopy of stable and transient species in a molecular beam

M. Tulej, M. Meisinger, G. Knopp, A. M. Walser, T. Gerber and P. P. Radi*

Department of General Energy, Paul Scherrer Institute, CH-5232 Villigen, Switzerland

Received 8 December 2006; Accepted 31 January 2007

A new apparatus is described that uses nonlinear and linear spectroscopic techniques simultaneously for the characterization of stable and transient molecules in a molecular beam environment. Short-lived species are generated by applying a well-defined discharge on a suitable precursor prior to supersonic expansion. Femtosecond ionization and mass spectrometry is used to optimize the discharge source. Degenerate and two-color resonant four-wave mixing spectroscopy (DFWM and TC-RFWM, respectively) are used in tandem with laser-induced fluorescence (LIF) and cavity ring-down spectroscopy (CRD). We demonstrate initial experiments on the 4051 Å band of C_3 ($\tilde{A}^1\Pi_u - \tilde{X}^1\Sigma_g^+$, 000–000). DFWM, LIF and CRD display similarities in the general shape and position of the rovibronic transitions. A more detailed view, however, reveals the complementary character of the methods and the potential of simultaneously measured spectra. High signal-to-noise ratios and well-structured spectra are obtained by DFWM. LIF is favorable for the observation of weak features but strongly dependent on the relaxation mechanism of the upper excited state. CRD suffers generally from a large background signal but yields quantitative information. By applying the methods in parallel, quantitative measurements of molecular number densities, transitions dipole moments and relaxation rates are accessible. **Copyright © 2007 John Wiley & Sons, Ltd.**

KEYWORDS: degenerate four-wave mixing; two-color resonant four-wave mixing; multiplex spectroscopy; C_3; discharge source; cavity ring-down; laser-induced fluorescence; molecular beam; transient species

INTRODUCTION

Degenerate four-wave mixing (DFWM) and two-color resonant four-wave mixing (TC-RFWM) are nonlinear spectroscopic tools exhibiting high signal-to-noise (S/N) ratios resulting from a fully resonant process. As a consequence, the methods are applicable to species that are present in low concentrations. This property has been successfully exploited for the detection of trace species in low pressure cells, flames and molecular beams.[1–13] These nonlinear techniques are usually complementary to linear spectroscopic methods and offer frequently advantageous capabilities. The coherent, laser-like signal beam ensures collection of the entire signal rather than a small fraction as compared to an incoherent process like Raman scattering or laser-induced fluorescence (LIF). In addition to the high collection efficiency, a coherent signal beam allows the rejection of stray light by remote probing. While linear absorption remains unique in terms of an overall simplicity, the generally weak signal needs to be extracted from a substantial and fluctuating baseline, rendering the method impracticable for low density environments. On the other hand, the background-free DFWM renders an absorption-like spectrum as well.[14,15] In fact, RFWM techniques are based on absorption and the signal intensity is insensitive to the lifetime of the upper energy level.[16] It has been demonstrated that the large and important category of molecules exhibiting non-fluorescing[17] or pre-dissociative states are accessible.[18–22] Another advantage of DFWM has been pointed out by Vaccaro and coworkers.[23,24] The method provides means for discriminating rovibronic branches by judicious selection of polarization characteristics of the input beams. Also, polarization schemes have been proposed that permit the selective detection of molecular orientation and alignment.[25]

The use of two distinct input frequencies for TC-RFWM provides an added benefit since the signal is obtained only when both frequencies interact with distinct molecular transitions that share a common level. TC-RFWM has been used for double-resonance spectroscopy of stable molecules in sample cells,[26–28] molecular beams[11,29] and flames.[4,30] The selectivity of the two-color technique by intermediate level labeling is advantageous for the simplification of spectrally

*Correspondence to: P. P. Radi, Department of General Energy, Paul Scherrer Institute, CH-5232 Villigen, Switzerland.
E-mail: peter radi@psi.ch

Copyright © 2007 John Wiley & Sons, Ltd.

WILEY InterScience® DISCOVER SOMETHING GREAT

congested regions. Furthermore, rotational characterization of high-lying vibrational states on the ground potential energy surface is feasible by the stimulated emission pumping (SEP) capabilities of TC-RFWM.[8,31] Conventionally, SEP experiments are accomplished by monitoring the depletion of the spontaneous fluorescence from the excited state (fluorescence dip, FD-SEP). However, similar to absorption spectroscopy, the main inconvenience of this method is that the signal of interest is detected as a weak depletion superimposed upon an often fluctuating fluorescence background. The nonlinear TC-RFWM exhibits inherently better S/N ratios owing to its background-free characteristic. However, the nonlinear method suffers from its quadratic dependence on number density and the cross-sections involved.[32]

Considering merits and limitations, Tobiason *et al*.[32] applied both nonlinear and linear SEP spectroscopy to investigate bound and resonance states of the HCO radical covering an energy range of 2000–21 000 cm^{-1}. FD-SEP has been favored in situations where weak or broad transitions are involved. In another study on pyrazine and pyridizine,[33] DFWM has been proven to be advantageous when the upper state relaxation mechanism is unfavorable for LIF detection. However, the fourth-order dependence on the Hönl–London factors[34–36] makes the detection of weak transitions inferior to the linear method for high-resolution spectroscopy.[33] Brock and Rohlfing applied TC-RFWM, LIF and dispersed fluorescence for a spectroscopic study of the jet-cooled vinoxy radical. From the difference between the TC-RFWM and LIF spectra and the measured lifetimes, a dramatic increase in the predissociation rate of the $\tilde{B}$ state at 1190 cm^{-1} above the origin has been observed.[37] Recently, DFWM spectra of the $B^3\Sigma^- - X^3\Sigma^-$ transition of SO have been recorded. These spectra have been combined with LIF and absorption and Fourier transform emission spectra to enable a rotational analysis and deperturbation of vibrational levels of the B state up to $v' = 16$.[18]

These examples show convincingly that the selection of the spectroscopic method is subtle and that a combination of different (linear and nonlinear) techniques is often beneficial for a detailed spectroscopic analysis. The *simultaneous* use of RFWM and one or more linear technique constitutes another class of powerful spectroscopy. In a pioneering work by Germann and Rakestraw, DFWM and absorption has been used in tandem (multiplex spectroscopy) to measure transition dipole moments and absolute concentrations of molecular species.[38] The method relies on the fact that these two forms of spectroscopy involve the same quantities but have a different functional dependence on the two variables of interest, i.e. transition dipole moment, μ_{12}, and the population difference in the ground and excited state, ΔN. In a similar way, DFWM and LIF can be combined to measure quantum-state-specific quenching rates. The different dependence on μ_{12} and ΔN for DFWM and LIF signal intensities has been exploited for multiplex spectroscopy of NO_2 in a molecular beam and yields relative line strength factors and the ratio of populations in different energy levels.[39] Also, the multiplexing of DFWM and LIF provided information on the transition dipole moment dependence of the DFWM process, even when the level populations are not accurately known.

Recently, we have performed photo-fragment excitation spectroscopy (PHOFEX) by multiplexing DFWM and LIF and have shown the substantial advantages of such an experimental setup for the study of unimolecular reaction dynamics. The method has been applied to investigate the radical channel decomposition of formaldehyde, i.e. $H_2CO \rightarrow H + HCO$.[15] The DFWM configuration is used to excite H_2CO to an energy level close to the threshold for dissociation and LIF is simultaneously employed to detect the nascent HCO fragments. The PHOFEX signals are subsequently referenced to the DFWM signals and yield relative fluorescence yields that reflect state-specific propensities of the dissociation reaction. However, the method relies on an accurate reduction of the DFWM intensities to number densities. Systematic investigations of DFWM signal intensities have been performed mostly on diatomic molecules[16,34–36,40] and only limited information is available for polyatomic molecules. To obtain more experimental data on the four-wave mixing signal dependence of an asymmetric top molecule, we have performed a combined study of DFWM and cavity ring-down (CRD) spectroscopy on jet-cooled formaldehyde.[14] CRD spectroscopy yields quantitative information on number densities in the molecular beam more directly than LIF. Unfortunately, the multiplexing of the two methods could not be achieved for this study since a complex experimental environment is required (*vide infra*). The comparative study has shown that the DFWM signal intensities are quadratically dependent on the number density and absorption cross-section for carefully controlled saturation conditions ($I \simeq I_{sat}$). However, since the CRD and DFWM experiments have been performed in succession, it is important to consider that expansion conditions in the molecular beam apparatus may differ slightly for different experiments. Even though backing pressure and H_2CO/seed gas mixtures are carefully controlled, a specific final rotational temperature is difficult to achieve and renders the comparison of the CRD and DFWM signal intensities less precise. The synchronized observation of the two methods is clearly preferable.

To explore the potential of multiplexing nonlinear and linear spectroscopy, we report in this work on the realization of a new apparatus that allows the *simultaneous* application of resonant four-wave mixing techniques (DFWM or TC-RFWM), LIF and CRD spectroscopy in a molecular beam environment. In addition, a discharge source is introduced providing access to supersonically cooled transient molecules and radicals. The precursors and optimal operating conditions for the discharge source are characterized *in situ* by femtosecond ionization and mass spectrometry

Copyright © 2007 John Wiley & Sons, Ltd.

DOI: 10.1002/jrs

with a connected reflectron time-of-flight tube. Initial multiplex experiments are demonstrated on the 4051 Å band of C_3 ($\tilde{A}^1\Pi_u - \tilde{X}^1\Sigma_g^+$, 000–000).

EXPERIMENTAL

Molecular beam apparatus and discharge source

Figure 1 depicts a schematic representation of the experimental setup. A molecular beam is generated by supersonic expansion through a pulsed valve which is mounted on an xyz-translation stage. For solid or liquid substances exhibiting a low vapor pressure, the source holder is resistively heatable in two stages by separate heating loops (thermocoax). For example, internally cold H_2CO can be obtained by heating a sample of solid *para*-formaldehyde (≈360 K) to liberate the monomer which is co-expanded with He at backing pressures behind the valve of ≈1.5 atm.[14,15] The valve operates at 10 Hz and creates a pulse of ≈500 μs duration. Transient species, like C_3, are produced by applying a discharge assembly containing a set of electrically isolated stainless steel disc electrodes mounted on the valve body by glass ceramic spacers (MACOR). A typical experimental procedure for C_3 production starts with a trigger to the solenoid valve to expand ≈5% of a precursor (acetylene or cyclopropane) diluted in Ar. At a variable time after the initial trigger for the valve, a well-defined high-voltage pulse of ≈800 V and adjustable duration is applied to the discharge electrodes. By changing the polarity of the discharge, the direction of the electrons to either co- or counter-propagation with respect to the molecular beam can be chosen. A careful optimization of the voltage, trigger delay, trigger duration and polarity yields an intense and remarkably stable molecular beam. Rotational temperatures strongly depend on these adjustable parameters and provide arbitrary rotational temperatures in the range of 10–100 K. It is noteworthy that similar discharge sources have been applied to generate a significant abundance of charged species and impart, therefore, means to access ions for spectroscopic characterization.[41] The molecular beam propagates into the vacuum chamber pumped by a 1400 l/s turbo pump (Pfeiffer TPH 1501P). During operation the source chamber is at a typical pressure of $\approx 10^{-2}$ Pa. Multiplex spectroscopy is performed perpendicular to the molecular beam and roughly 2 cm downstream from the nozzle/discharge exit.

Nonlinear spectroscopy: DFWM and TC-RFWM

The DFWM and TC-RFWM setup is outlined only briefly because detailed descriptions have been published elsewhere.[4,6] One or two separately pumped dye lasers (narrowscan, Radiant Dyes) are used for DFWM and TC-RFWM, respectively. Both dye lasers are equipped with second-harmonic generation options. The specified bandwidth of the systems is ≈0.02 cm^{-1}. The quantitative reduction of RFWM signals to population densities in the molecular beam requires careful control of the laser beam intensities. Therefore, the pulse energies are arbitrarily adjustable with a variable attenuator (Newport, M-935-10) and range typically from ≈1 nJ to a few millijoules per pulse depending on the molecular transitions involved. For the applied nonlinear methods (as well as for CRD, *vide infra*), a very homogeneous

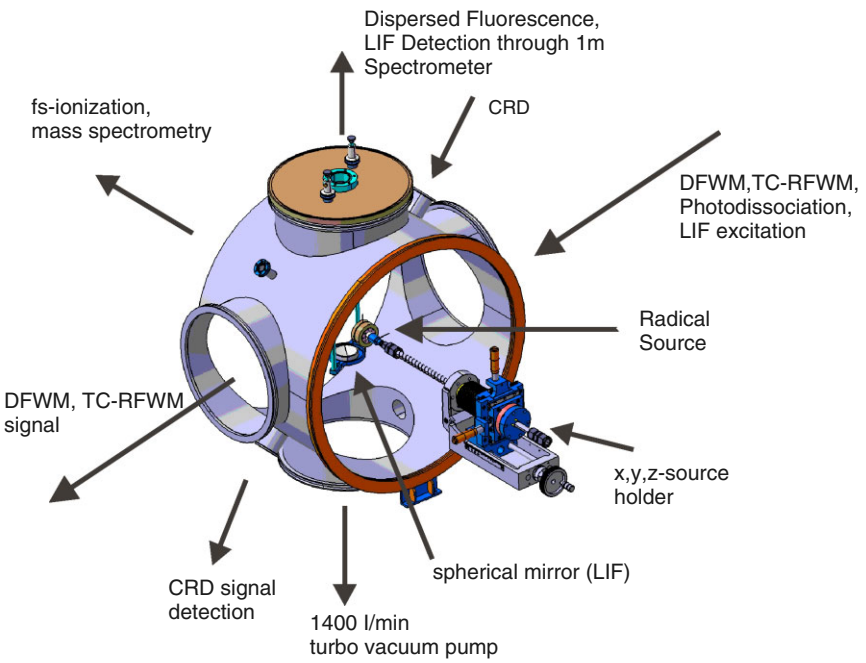

Figure 1. Molecular beam apparatus for multiplex spectroscopy. See text for details. This figure is available in colour online at www.interscience.wiley.com/journal/jrs.

Copyright © 2007 John Wiley & Sons, Ltd.

DOI: 10.1002/jrs

intensity distribution over the entire laser beam diameter is required. Therefore, the laser beams have been spatially filtered by 50 or 100 μm pinholes and a series of apertures over a path of approximately 2 m. A combination of optical components establishes a forward BOXCARS configuration.[4,6] The three input beams with wave vectors $\boldsymbol{k_1}$, $\boldsymbol{k_2}$ and $\boldsymbol{k_3}$ generate a signal beam wave vector $\boldsymbol{k_4}$ which is defined by the phase-matching condition, $\boldsymbol{k_1} + \boldsymbol{k_3} = \boldsymbol{k_2} + \boldsymbol{k_4}$. Polarization rotators are introduced in the path of the three beams and produce an arbitrary configuration of the unit polarization vectors, $\boldsymbol{\varepsilon_n}$, $n = (1, 2, 3, 4)$ of the electric fields. The polarization geometry is conventionally[42] specified as $\boldsymbol{\varepsilon_4\varepsilon_1\varepsilon_3\varepsilon_2}$ (e.g. YYYY, YXYX, etc.) assuming the laser wave vectors to be in nearly collinear phase-matching geometry. The parallelized incident laser beams pass a quartz convex lens ($f = 1000$ mm) and are focused through a window into the molecular beam interaction region. For the double-resonance experiment, one of the three incident beams ($\boldsymbol{k_2}$) is replaced by a laser beam of a different frequency (PROBE beam) to establish the forward BOXCARS configuration for TC-RFWM[4,8,29,43]. The equal frequency input beams ($\boldsymbol{k_1}$ and $\boldsymbol{k_3}$) are commonly referred to as PUMP beams.

The four-wave mixing signal is re-collimated by a second quartz lens ($f = 1000$ mm) and passes through a polarization beam splitter which is adjusted to transmit only the signal beam polarization given by the phase-matching condition. Then it is allowed to propagate roughly 3 m through several irises and optical and spatial filters to remove interfering scattered light and unwanted fluorescence. Further reduction of stray light is achieved by a spatial filter consisting of a 30 mm focal length lens and a 50 μm pinhole in front of the photomultiplier tube. The substantial S/N ratios demand a photomultiplier tube (PMT) with a large dynamic range (Hamamatsu H3177). Furthermore, high signal intensities observed occasionally in this experiment require neutral density filters up to ND5 in front of the PMT.

Linear spectroscopy: LIF and CRD

LIF originating from the RFWM beams or, alternatively, from a separately introduced excitation laser is collected at right angles to both the molecular beam and laser beam propagation by a spherical aluminum mirror (diameter 60 mm, $r = 50$ mm, $f/25$) (Fig. 1). Subsequently, the parallel LIF beam is focused onto the slit of a 1 m length monochromator and detected by a PMT.

The CRD configuration is based on a commercial design (Los Gatos). The optical cavity consists of a set of dielectric-coated mirrors with reflectivities of >99.9% in the UV and >99.995% in the visible. The mirrors are mounted on the molecular beam apparatus such that the closed cavity path is aligned perpendicular to the molecular beam propagation and forms an angle of ≈45° with both the four-wave mixing beams and the fluorescence signal beam. A three-point micrometer mount for each mirror allows alignment of the cavity. The cavity length is ≈1 m and the path intersects the free jet in the vicinity of the interaction region of the four-wave mixing and LIF excitation beams. In general, a 5% reflection of the laser beam from a window or prism is sufficient for CRD spectroscopy. A small fraction of this beam (0.1 to 0.005%) is injected by transmission through the first mirror into the cavity where its amplitude decays as the pulses oscillate within the resonator. The weakly transmitted beam through the end mirror passes through a frequency filter to reject stray light and is detected by a fast PMT. The decay transient is typically averaged over 20–30 laser pulses on a digital oscilloscope (LeCroy LC564A) and transferred to a PC where a single exponential fit to the waveform is performed. An accurate absorption spectrum is obtained by measuring the ring-down time *vs* wavelength and taking into account losses experienced by the light pulse inside the cavity due to mirror reflectivity and mirror absorption, optical scattering and molecular absorption.[14]

Femtosecond ionization and mass spectrometry

As mentioned above, the production of transient species in the molecular beam by applying the discharge assembly requires careful optimization of the experimental conditions. For this purpose femtosecond ionization is particularly advantageous. The ultrashort pulse width combined with the high intensity (≈10^{15} Watt cm^{-2}) of the light source permits excitation to the ionization state on a time scale which competes with nuclear motion. The electric field generated by the laser pulse is $E_0 = (\sqrt{2I/c\varepsilon_0})$, where E_0 is the electric field strength (in V m^{-1}), I is the intensity of the laser beam (in W m^{-2}), ε_0 is the permittivity of free space and c is the speed of light. Thus, the laser intensity corresponds to an electric field strength of ≈8.7 V Å^{-1} which is sufficient to ionize most of the molecules.[44] The Ti : sapphire laser system makes use of the chirped pulse amplification (CPA) technique and produces bandwidth-limited output pulses of ≈100 fs and a bandwidth of 9 nm. Typical pulse energies are 250 μJ at a wavelength centered around 780 nm. The femtosecond pulses are focused into the ionization region of the source chamber to a diameter of <20 μm and intersect the supersonic molecular beam containing the neutral species produced by the radical source. The ions formed in the ionization process are accelerated in an electric field and directed through the first field-free region toward the reflector. Ions are then reflected and travel through the second field-free region and are detected by a microchannel plate detector. The resolution of the mass spectrometer, $m/\Delta m$, is typically 3000 at $m/z = 200$, where m is the mass of the ion in atomic mass units (amu) and z its charge number.

RESULTS AND DISCUSSION

Radical source characterization by femtosecond ionization mass spectrometry

Conventional mass spectrometry is widely used to characterize molecular beams. Ionization by electron impact is,

Copyright © 2007 John Wiley & Sons, Ltd.

DOI: 10.1002/jrs

however, unfavorable because of the known problem of collision-induced fragmentation. The mass spectrum in this case does not represent the mass distribution of the neutral molecules in the beam. Alternatively, single photo-ionization (SPI) by nanosecond laser pulses in the VUV (>10 eV) can be applied to ionize a large number of species to yield molecular ions without fragmentation. However, SPI with VUV photons is a technically demanding method and requires knowledge of the ionization threshold. Multiphoton ionization (MPI) in the visible or UV leads in general to strong fragmentation.[45] An excitation to the intermediate state will distribute energy into internal degrees of freedom and possibly dissociate within nanoseconds before the ionization step takes place. On the other hand, mass spectra recorded with ultrashort laser pulses are generally not affected by unimolecular dissociation and therefore are better suited for the production of an intact molecular ion from a neutral parent.[44,46,47] Figure 2a displays a mass spectrum obtained by fs-ionization of ≈5% cyclopropane co-expanded in Ar at 1.5 atm backing pressure. The substantial stability of this molecular ion produces one major peak at $m/z = 42$, even at the highest ionization intensities provided by our laser system. The losses of up to three hydrogen atoms is observed but essentially negligible. For comparison, a typical mass spectrum of cyclopropane is shown in Fig. 2b which has been obtained by electron impact ionization (70 eV).[48] In addition to the parent ion, a large number of fragments are observed owing to the substantial excess energy deposited in the parent ion. Figure2c depicts the fs-ionization mass spectrum of the cyclopropane precursor when applying the high-voltage pulse to the discharge assembly. The graphic clearly demonstrates the production of several carbon clusters, C_n, $n \leq 7$ and their corresponding hydrogenated complements in the discharge source. The ions are mainly formed from the neutral molecules emerging from the source even though a small contribution from the dissociation of small hydrocarbon ions following the field ionization mechanism cannot be excluded completely.[46,49] In general, however, the ultrafast ionization displays – at appropriate laser intensities – qualitatively the primary distribution of the neutral parents in the beam and is a valuable tool for the characterization and optimization of the discharge source. Note however, that a direct quantification of the mass spectra is difficult because the ionization cross-sections for fs-ionization may vary for each species. In addition to cyclopropane, several other hydrocarbon molecules have been tested with the discharge source. Most of these precursors produce large samples of various radicals and clusters. For these preliminary studies below, we focus on the carbon trimer. C_3 is an example of a short-lived species and plays an important role in the formation of soot particles in fuel-rich combustion processes.[50] In addition, the smallest polyatomic carbon chain is relevant for the chemistry of interstellar space and has been detected in many cometary spectra and recently identified in interstellar clouds.[51] In the following, we used a small percentage of acetylene diluted in 1.5 atm Ar as a simple and efficient precursor for the jet-cooled carbon trimer.

Another important feature of the discharge assembly is characterized in this work by spectroscopic means: the internal energy of the species emerging from the discharge source. Below, we demonstrate on C_3 that typical rotational temperatures of small polyatomic molecules of ≈60 K are achieved routinely and yield simplified spectra owing to the moderate rotational level population in the ground state.

Multiplex spectroscopy of C_3

Figure 3 depicts LIF, CRD and DFWM traces for the 4051 Å band of C_3 ($\tilde{A}^1\Pi_u - \tilde{X}^1\Sigma_g^+$, 000–000). The spectra have been observed simultaneously and demonstrate clearly the applicability of the methods for multiplex spectroscopy in the low-density environment of a molecular beam. Substantial sensitivities are observed for the linear and nonlinear spectroscopic techniques, although the latter method is subject to a reduced sensitivity due to a greater than linear dependence on number density. In fact, the square root of the DFWM signal is shown in the figure. Recent investigations in this laboratory[14] and by several other groups[16,52–55] have shown that for the carefully controlled conditions of this experiment (i.e. collision-free environment of the molecular beam, laser intensity, polarization of the input beams) the DFWM signal expression is given by the relation:

$$I_{\mathrm{DFWM}} \propto (N'')^2(\sigma_{\mathrm{ge}})^2 \quad (1)$$

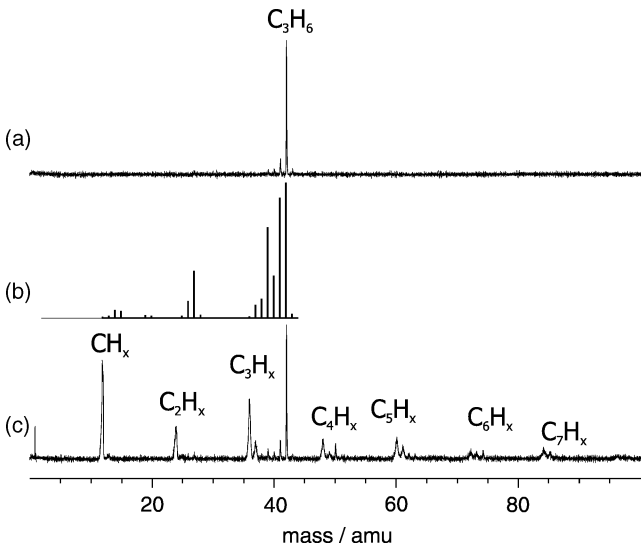

Figure 2. Characterization of the discharge source by fs-ionization mass spectrometry. Five percent cyclopropane is expanded in Ar seed gas at a backing pressure of ≈1.5 atm. (a) Discharge source off, (b) typical mass spectra of cyclopropane obtained by using electron impact ionization (70 eV) for comparison (Ref 48) and (c) discharge source on. The discharge applied on the precursor prior to the supersonic expansion produces several hydrocarbons with the general formula C_nH_x.

Copyright © 2007 John Wiley & Sons, Ltd.

DOI: 10.1002/jrs

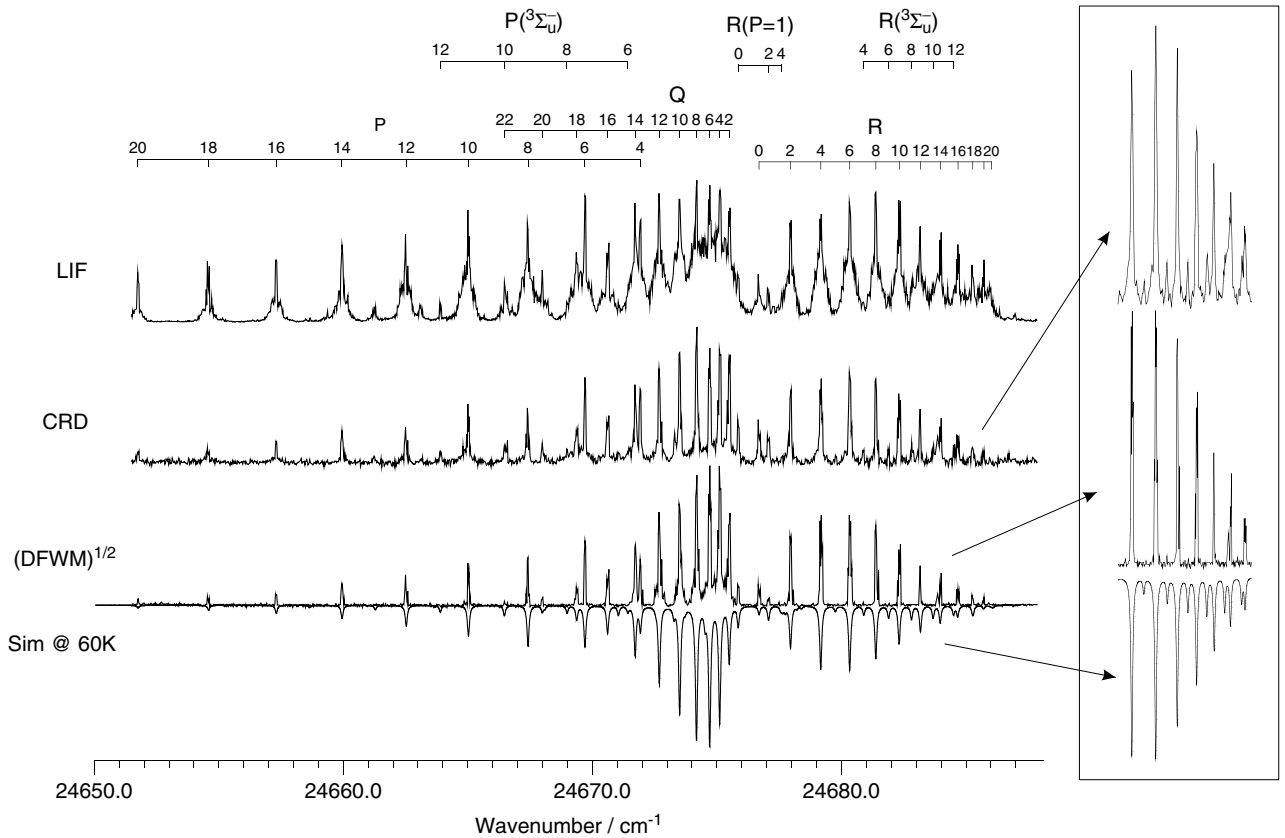

Figure 3. Multiplex spectroscopy of the $\tilde{A}^1\Pi_u - \tilde{X}^1\Sigma_g^+$, 000–000 transition of C_3 by applying DFWM, CRD and LIF simultaneously. The square root of the DFWM signal is shown, which represents the functional dependence of the method on number density and transition dipole moment. The spectrum is simulated by an asymmetric rotor model for a rotational temperature of 60 K (lowest trace, inverted). The inset displays an expanded ordinate for the CRD, DFWM and simulated traces. Weak features in the spectrum due to perturbations ($P(^3\Sigma_u^-)$, $R(P = 1)$ and $R(^3\Sigma_u^-)$) are suppressed by the DFWM method while intense zero-order transitions (P,Q,R) appear enhanced. See text for details.

Here, σ_{ge} refers to the absorption cross-section between ground and excited state and N'' to the ground state population. Thus, considering Eqn 1, the square root of the DFWM signal intensities is directly comparable to the CRD absorption spectra. Indeed, a rather excellent agreement between the quantitative CRD method and the highly sensitive, nonlinear DFWM technique is observed, which verifies the applicability of Eqn 1. Our experimental implementation of the techniques yields mostly a superior S/N ratio for the background-free DFWM technique. By using neutral density filters in front of the PMT, S/N ratios of up to 50 000 could be inferred for the carbon trimer. It is, however, important to indicate that alignment and optimization of the signal for the nonlinear method is considerably more complex than for LIF or absorption spectroscopy.

The LIF signal originating from excitation by the three DFWM input beams in the interaction region is shown in the upper trace of Fig. 3. As mentioned in the 'Experimental' section, the fluorescence signal is collected and imaged onto the entrance of a monochromator which acts as a bandpass filter. To optimize the frequency and collection efficiency of the spectrometer, dispersed fluorescence (DF) spectra are measured for selected rovibronic excitations. Figure 4 shows a typical DF scan obtained upon excitation of the Q(4) line of the $\tilde{A}^1\Pi_u - \tilde{X}^1\Sigma_g^+$, 000–000 band of C_3 at 24 675.1 cm^{-1} (Fig. 3). The abscissa is the wavenumber shift from the exciting line. The assignment of the vibronic bands is performed by using vibrational constants for ν_1 and ν_2 from the literature.[56] The progressions are indicated by $0\nu0$ and $1\nu0$ with ($\nu = 0, 2, 4\ldots$). The excitation scan in Fig. 3 is recorded by tuning the spectrometer to the 020 band center and collecting the fluorescence by opening the entrance slit to ≈3 mm, yielding a band pass of ≈10 cm^{-1} which is sufficient to suppress stray light efficiently from the excitation frequency. The LIF spectrum displays substantial power broadening since excitation is provided by the DFWM input beams which are adjusted by the variable attenuator to meet the saturation conditions for the nonlinear process ($I \simeq I_{sat}$).

Copyright © 2007 John Wiley & Sons, Ltd.

DOI: 10.1002/jrs

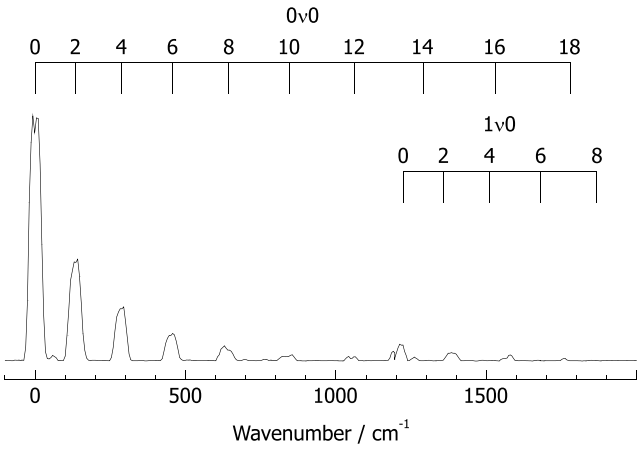

Figure 4. Dispersed fluorescence upon excitation of the Q(4) transition at 24675.1 cm^{-1}. Progressions are indicated by $0\nu0$ and $1\nu0$ with ($\nu = 0, 2, 4 \ldots$).

Alternatively, multiplex spectroscopy by simultaneous application of the two linear methods CRD and LIF exclusively can be used to reduce the effects of optical saturation. In this case, the DFWM input beams are blocked and LIF is generated by the low-intensity laser pulses inside the high-reflecting mirrors of CRD setup. A typical result is depicted in Fig. 5. The effects of optical saturation of the LIF transitions are strongly suppressed and the spectra display much narrower features while preserving an excellent S/N ratio. Although a direct comparison of LIF *vs* DFWM spectra is not possible in this experiment, the CRD data can be used as a reference for sequentially performed multiplex experiments.

The inverted trace at the bottom of Fig. 3 shows, in addition, a spectral simulation by using the PGOPHER program package, developed by Western,[57] and using molecular constants from the literature.[58–60] For the synthetic spectrum a rotational temperature of 60 K has been assumed. Considerable theoretical and experimental work has been dedicated to the C_3 ground and electronically excited states. The $\tilde{A}^1\Pi_u - \tilde{X}^1\Sigma_g^+$, 000–000 transition has been assigned by Gausset *et al*.[60] in the mid-60's. The analysis of new high-resolution data obtained by Saykally and coworkers[61] has led to the reassignment of the R(0) transition at 24676.70 cm^{-1} but failed to identify several transitions in the CRD spectrum. Very recent Fourier transform emission spectra implied that some of the extra transitions are caused by an unknown perturbing state.[62] Finally, laser-induced fluorescence excitation spectra at different time gatings for detection have been reported by Zhang *et al*.[58] The authors found at least two states perturbing the $\tilde{A}^1\Pi_u$, 000 state. Fluorescence decay measurements of the main band gave single exponential decays with lifetimes of 192–227 ns. The perturbing states gave bi-exponential decays with much longer lifetimes. One of these perturbing states has been assigned to a $^3\Sigma_u^-$ vibronic state and the other to a $P = 1$ state.

Some of the extra transitions of the P($^3\Sigma_u^-$), R($^3\Sigma_u^-$) and R($P = 1$) branches are weak but clearly observed in the CRD and LIF spectra (Figs 3 and 5). On the other hand, these weak features are significantly suppressed by the four-wave mixing process, while an enhancement is observed for the strong transitions to the zero order ($\tilde{A}^1\Pi_u$, 000) levels. This characteristic behavior of the nonlinear

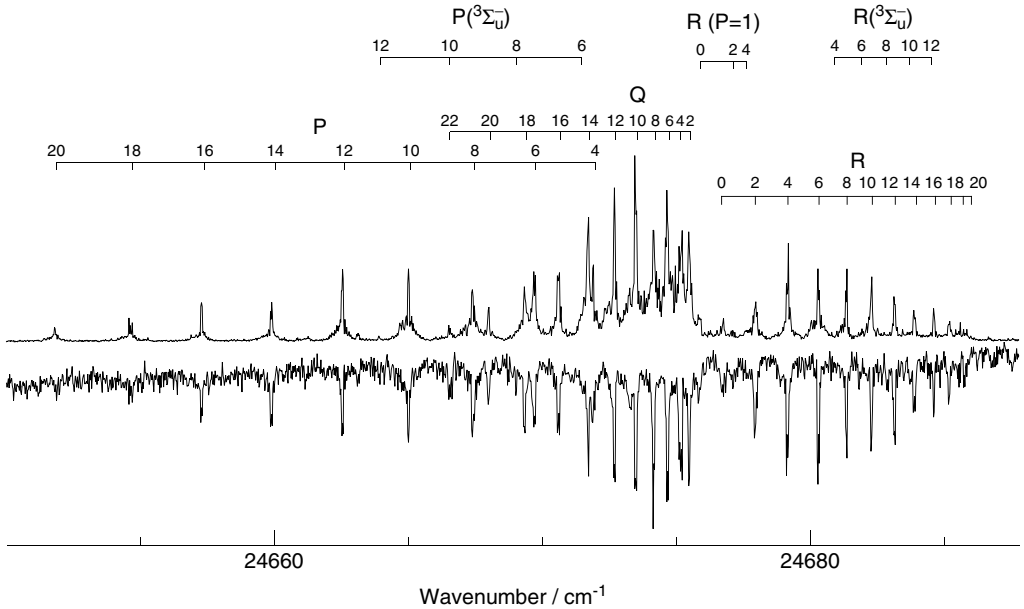

Figure 5. Multiplex spectroscopy by applying CRD (lower, inverted) and LIF (upper). LIF is obtained by the low-intensity laser used for CRD spectroscopy only. The DFWM input beams are blocked. This configuration reduces power broadening effects in the LIF spectrum substantially.

Copyright © 2007 John Wiley & Sons, Ltd.

DOI: 10.1002/jrs

technique increases the overall resolution and leads to a more structured spectrum.

Another method is available for the newly implemented experimental configuration that simplifies dramatically congested and complex spectra which are often encountered for polyatomic molecules and radicals. The use of two separate input frequencies for four-wave mixing provides an added advantage because a signal is obtained only when both frequencies interact with distinct molecular transitions simultaneously. Figure 6 depicts the multiplex traces of the $\tilde{A}^1\Pi_u - \tilde{X}^1\Sigma_g^+$, 000–000 transition of C_3 by LIF and TC-RFWM. In addition, the spectral simulation is shown for comparison (lower trace, inverted). For the TC-RFWM spectra, the PUMP laser is tuned to overlap with the (unperturbed) R(4) at 24 679 cm^{-1} exciting molecules with the total angular momentum $J'' = 4$ in the ground electronic $\tilde{X}^1\Sigma_g^+$ state to $J' = 5$ in the excited $\tilde{A}^1\Pi_u$ state. Scanning the frequency of the PROBE laser in the range of the $\tilde{A}^1\Pi_u - \tilde{X}^1\Sigma_g^+$, 000–000 band reveals four major transitions only, which are, in general, unambiguously assignable since they are required to share a common level with the PUMP transition. The two double-resonance processes involved are (1) stimulated emission pumping (SEP) involving the same upper state ($J' = 5$) and (2) upward transitions (UP) due to depletion of the ground state population. Two major UP transitions are observed for P(4) and Q(4) at 24 672 and 24 675 cm^{-1}, respectively, and one SEP transition for P(6) at 24 669.7 cm^{-1}. All PROBE transitions are well isolated and their spectral position is readily determinable. A comparison of the TC-RFWM spectrum in Fig. 6 with the DFWM trace in Fig. 3 demonstrates the potential to simplify the assignments and to increase the accuracy of the line position determinations.

The LIF trace in Fig. 6, which has been recorded simultaneously, shows the major features of the 000–000 band but is afflicted with substantial noise. In fact, significant fluorescence is produced by the PUMP lasers fixed on the P(4) transition, yielding a constant background and reducing the S/N ration to ≈2. On the other hand, the constant fluorescence background indicates sensitively the stability of the experimental conditions (i.e. supersonic expansion, discharge source, laser stability).

CONCLUSIONS

A new apparatus for multiplexing linear and nonlinear spectroscopic methods for the investigation of stable and transient molecules in a free-jet expansion is presented. Reactive species are generated from a suitable precursor

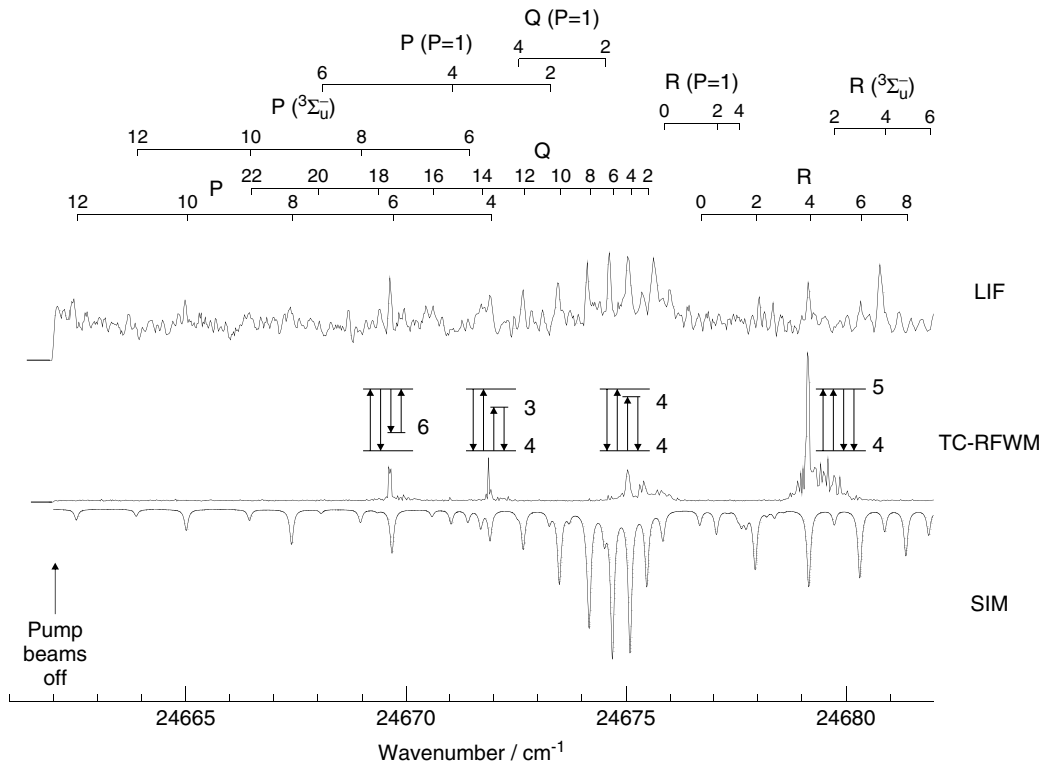

Figure 6. Multiplex spectroscopy by applying TC-RFWM (lower) and LIF (upper). The PUMP laser is tuned to the R(4) transition at 24 679 cm^{-1} while the PROBE laser is scanned in the range of the 000–000 band. A dramatic simplification of the one-color spectrum is observed and assigned in a straightforward manner. Two major UP transitions are observed for P(4) and Q(4) at 24 672 and 24675 cm^{-1} and one SEP transition for P(6) at 24 669.7 cm^{-1}. Significant noise in the LIF spectrum is observed due to the PUMP laser and reduces the S/N to ≈2. The simulated spectrum is shown inverted for comparison.

Copyright © 2007 John Wiley & Sons, Ltd.

DOI: 10.1002/jrs

by applying a well-defined high-voltage discharge prior to supersonic expansion. Selection of the precursor and optimization of the source is achieved by *in situ* femtosecond ionization and mass spectrometric analysis of the species present in the molecular beam.

To characterize and explore the potential of simultaneous measurements of four-wave mixing, CRD and LIF spectra, initial experiments are performed on the carbon trimer which is generated by using acetylene diluted in Ar as a precursor for the discharge source. The $\tilde{A}^1\Pi_u - \tilde{X}^1\Sigma_g^+$, 000–000 transition of C_3 exhibits strong zero-order features and weak lines due to perturbations by near lying electronic states. In addition, lifetimes of the rotational levels in the upper state $\tilde{A}^1\Pi_u$ vary widely. The comparison of the three methods (Fig. 3) reveals expected similarities in the general shape and position of rovibronic patterns. For DFWM, significantly better S/N ratios are observed owing to the background-free nature of the method. The method clearly exhibits more sharply resolved peaks and less overall congestion than its linear counterparts. These distinctions stem mainly from the nonlinear character of the four-wave mixing process leading to a quadratic dependence on number density and transition dipole moment (Eqn 1). The reduction of signal intensities to relative number densities requires, however, careful control of the saturation conditions, which is often difficult to achieve for a spectrum exhibiting large variations of the oscillator strengths. The parallel observation of absorption spectra by CRD spectroscopy provides the means to quantify the molecular number density and is, therefore, complementary to DFWM spectroscopy. Clearly, CRD spectra suffer from a lower sensitivity and supply substantially inferior resolution spectroscopic data. Nevertheless, the weak features in the 4051 Å band of C_3 are discernible owing to the method's linear dependence on the transition dipole moment. Similarly, LIF is favorable for the detection of weak features in the spectrum. Its high sensitivity and relatively simple experimental setup renders the method often advantageous with respect to its nonlinear counterparts. However, LIF is strongly dependent on the upper state relaxation mechanism. Excitations to the long-lived upper states in the C_3 spectrum are observable weakly for long time gatings only, but are clearly present in the CRD spectra. Simplification and straightforward assignment of complex spectra is achieved by intermediate labeling using the double-resonant variant of four-wave mixing. By tuning the PUMP laser to a specific rotational transition and scanning the PROBE, congested regions in the C_3 spectrum are reduced to a few transitions.

The simultaneous application of the techniques provides information that are inaccessible by other means. For example, multiplex spectroscopy can be used to determine quantities such as transition dipole moment, number density and excited quenching rate since the techniques exhibit different functional dependence of the signal intensities on these parameters. Also, in a recent work, we have shown that dynamic information is attainable by using a DFWM setup to excite molecules to a pre-dissociative level and observing the fragment by LIF.[15] Photo-fragment quantum yields of H_2CO are obtained by referencing LIF signal intensities with DFWM spectra. Additional information by simultaneously observed CRD will remove ambiguities due to saturation effects in DFWM, in particular for weak transitions where the condition $I \simeq I_{sat}$ is difficult to achieve.

Acknowledgements

The authors wish to thank C. M. Western for his support for the simulation of the C_3 spectra including perturbation by two electronic states. This work is supported by the Swiss Federal Office of Energy and the Swiss National Science Foundation.

REFERENCES

1. Ewart P, O'Leary S. *Opt. Lett.* 1986; **11**: 279.
2. Farrow R, Rakestraw D. *Science* 1992; **257**: 1894.
3. Vaccaro P. In *Nonlinear Spectroscopy for Molecular Structure Determinatiom*, Hirota FRMJ, Tsuchiya EandS (eds). Blackwell Scientific: London, 1998; 75.
4. Radi PP, Frey HM, Mischler B, Tzannis AP, Beaud P, Gerber T. *Chem. Phys. Lett.* 1997; **265**: 271.
5. Radi PP, Beaud P, Frey HM, Gerber T, Mischler B, Tzannis AP. *Chimia* 1997; **51**: 771.
6. Radi PP, Mischler B, Schlegel A, Tzannis AP, Beaud P, Gerber T. *Combust. Flame* 1999; **118**: 301.
7. Hemmerling B, Radi P, Stampanoni-Panariello A, Kouzov A, Kozlov D. *C.R. Acad. Sci.*, Paris, 2001; **2**: 1001.
8. Radi PP, Tulej M, Knopp G, Beaud P, Gerber T. *J. Raman Spectrosc.* 2003; **34**: 1037.
9. Butenhoff T, Rohlfing E. *J. Chem. Phys.* 1993; **98**: 5460.
10. Butenhoff T, Rohlfing E. *J. Chem. Phys.* 1993; **98**: 5469.
11. Williams S, Tobiason JD, Dunlop JR, Rohlfing EA. *J. Chem. Phys.* 1995; **102**: 8342.
12. Lee KW, Lee KS, Jung KH, Volp HR. *J. Chem. Phys.* 2002; **117**: 9266.
13. Lee KW, Kim DC, Jung KH, Hahn JW. *J. Chem. Phys.* 1999; **111**: 1427.
14. Tulej M, Meisinger M, Knopp G, Walser A, Beaud P, Gerber T, Radi P. *J. Raman Spectrosc.* 2006; **37**: 376.
15. Tulej M, Knopp G, Beaud P, Gerber T, Radi PP. *J. Raman Spectrosc.* 2005; **36**: 109.
16. Farrow RL, Rakestraw DJ, Dreier T. *J. Opt. Soc. Am. B: Opt. Phys.* 1992; **9**: 1770.
17. Dunlop JR, Rohlfing EA. *J. Chem. Phys.* 1994; **100**: 856.
18. Liu CP, Elliott NL, Western CM, Lee YP, Colin R. *Journal of Molecular Spectroscopy* 2006; **238**: 213.
19. Liu CP, Reid SA, Lee YP. *J. Chem. Phys.* 2005; **122**: 124313.
20. Liu CP, Matsuda Y, Lee YP. *J. Chem. Phys.* 2003; **119**: 12335.
21. Li XH, Lee YP. *J. Chem. Phys.* 1999; **111**: 4942.
22. Li XH, Kumar A, Hsiao CC, Lee YP. *J. Phys. Chem. A* 1999; **103**: 6162.
23. Muller T, Wasserman TAW, Vaccaro PH, Johnson BR. *J. Chem. Phys.* 1998; **108**: 4.
24. Bracamonte A, Vaccaro P. *J. Chem. Phys.* 2003; **119**: 887.
25. Wasserman TAW, Vaccaro PH, Johnson BR. *J. Chem. Phys.* 1998; **108**: 7713.
26. Ashfold MNR, Chandler IW, Hayden CC, Mckay RI, Heck AJR. *Chem. Phys.* 1995; **201**: 237.
27. Buntine MA, Chandler DW, Hayden CC. *J. Chem. Phys.* 1992; **97**: 707.
28. Mccormack EF, Pratt ST, Dehmer PM, Dehmer JL. *Chem. Phys. Lett.* 1993; **211**: 147.

Copyright © 2007 John Wiley & Sons, Ltd.

29. Tulej M, Meisinger M, Knopp G, Walser AM, Beaud P, Gerber T, Radi PP. *J. Raman Spectrosc.* 2006; **37**: 680.
30. Hung WC, Huang ML, Lee YC, Lee YP. *J. Chem. Phys.* 1995; **103**: 9941.
31. Zhang Q, Kandel SA, Wasserman TAW, Vaccaro PH. *J. Chem. Phys.* 1992; **96**: 1640.
32. Tobiason JD, Dunlop JR, Rohlfing EA. *J. Chem. Phys.* 1995; **103**: 1448.
33. Li HZ, Dupre P, Kong W. *Chem. Phys. Lett.* 1997; **273**: 272.
34. Abrams R, Lind R. *Opt. Lett.* 1978; **2**: 94.
35. Williams S, Zare RN, Rahn LA. *J. Chem. Phys.* 1994; **101**: 1093.
36. Williams S, Zare RN, Rahn LA. *J. Chem. Phys.* 1994; **101**: 1072.
37. Brock LR, Rohlfing EA. *J. Chem. Phys.* 1997; **106**: 10048.
38. Germann GJ, Rakestraw DJ. *Science* 1994; **264**: 1750.
39. Tang Y, Reid SA. *Chem. Phys. Lett.* 1998; **292**: 691.
40. Pender J, Hesselink L. *Opt. Lett.* 1985; **10**: 264.
41. Tulej M, Kirkwood DA, Maccaferri G, Dopfer O, Maier JP. *Chem. Phys.* 1998; **228**: 293.
42. Williams S, Rohlfing EA, Rahn LA, Zare RN. *J. Chem. Phys.* 1997; **106**: 3090.
43. Radi PP, Kouzov AP. *J. Raman Spectrosc.* 2002; **33**: 925.
44. Dewitt MJ, Levis RJ. *J. Chem. Phys.* 1995; **102**: 8670.
45. Martin WB, Omalley RM. *Int. J. Mass Spectrom. Ion Processes* 1989; **95**: 39.
46. Levis RJ, DeWitt MJ. *J. Phys. Chem. A* 1999; **103**: 6493.
47. Willey KF, Brummel CL, Winograd N. *Chem. Phys. Lett.* 1997; **267**: 359.
48. Stein S. *''Mass Spectra'' by NIST Mass Spec Data Center, NIST Chemistry WebBook, NIST Standard Reference Database Number 69*. National Institute of Standards and Technology: Gaithersburg, MD, 2005; 20899.
49. Castillejo M, Couris S, Koudoumas E, Martin M. *Chem. Phys. Lett.* 1999; **308**: 373.
50. Kaiser RI, Le TN, Nguyen TL, Mebel AM, Balucani N, Lee YT, Stahl F, Schleyer PV, Schaefer HF. *Faraday Discuss.* 2001; **119**: 51.
51. Maier JP, Lakin NM, Walker GAH, Bohlender DA. *Astrophys J.* 2001; **553**: 267.
52. Dreier T, Rakestraw D. *Appl. Phys. B* 1990; **50**: 479.
53. Dreier T, Rakestraw DJ. *Opt. Lett.* 1990; **15**: 72.
54. Lee KW, Kim D-C, Jung K-H, Hahn J. *J. Chem. Phys.* 1999; **111**: 1427.
55. Derose P, Dai HL, Cheng PY. *Chem. Phys. Lett.* 1994; **220**: 207.
56. Rohlfing EA. *J. Chem. Phys.* 1989; **91**: 4531.
57. PGOPHER, a Program for Simulating Rotational Structure, C.M. Western, University of Bristol. http://pgopher.chm.bris.ac.uk, 2005.
58. Zhang GQ, Chen KS, Merer AJ, Hsu YC, Chen WJ, Shaji S, Liao YA. *J. Chem. Phys.* 2005; **122**: 244308.
59. Gendriesch R, Pehl K, Giesen T, Winnewisser G, Lewen F. *Z. Naturforsch., A: Phys. Sci.* 2003; **58**: 129.
60. Gausset L, Herzberg G, Lagerqvi. A, Rosen B. *Astrophysics J.* 1965; **142**: 45.
61. McCall BJ, Casaes RN, Adamkovics M, Saykally RJ. *Chem. Phys. Lett.* 2003; **374**: 583.
62. Tanabashi A, Hirao T, Amano T, Bernath PF. *Astrophys J.* 2005; **624**: 1116.

Copyright © 2007 John Wiley & Sons, Ltd.